

# Magnetic properties of the quasi-two-dimensional $S=\frac{1}{2}$ Heisenberg antiferromagnet $[\text{Cu}(\text{pyz})_2(\text{HF}_2)]\text{PF}_6$

E. Čížmár,<sup>1,2</sup> S. A. Zvyagin,<sup>1</sup> R. Beyer,<sup>1</sup> M. Uhlarz,<sup>1</sup> M. Ozerov,<sup>1</sup> Y. Skourski,<sup>1</sup> J. L. Manson,<sup>3</sup> J. A. Schlueter,<sup>4</sup> and J. Wosnitza<sup>1</sup>

<sup>1</sup>*Hochfeld-Magnetlabor Dresden (HLD), FZ Dresden-Rossendorf, D-01314 Dresden, Germany*

<sup>2</sup>*Centre of Low Temperature Physics, P. J. Šafárik University, SK-041 54 Košice, Slovakia*

<sup>3</sup>*Department of Chemistry and Biochemistry, Eastern Washington University, Cheney, Washington 99004, USA*

<sup>4</sup>*Materials Science Division, Argonne National Laboratory, Argonne, Illinois 60439, USA*

(Received 16 November 2009; published 22 February 2010)

We report on high-field magnetization, specific heat, and electron-spin-resonance (ESR) studies of the quasi-two-dimensional spin- $\frac{1}{2}$  Heisenberg antiferromagnet  $[\text{Cu}(\text{pyz})_2(\text{HF}_2)]\text{PF}_6$ . The frequency-field diagram of ESR modes below  $T_N=4.38$  K is described in the frame of the mean-field theory, confirming a collinear magnetic structure with an easy-plane anisotropy. The obtained results allowed us to determine the anisotropy/exchange interaction ratio,  $A/J=0.003$ , and the upper limit for the interplane/intraplane exchange interaction ratio,  $J'/J=1/16$ . It is argued that despite the onset of three-dimensional long-range magnetic ordering the magnetic properties of this material (including high-magnetic-field magnetization and nonmonotonic field dependence of the Néel temperature) are strongly affected by two-dimensional spin correlations.

DOI: [10.1103/PhysRevB.81.064422](https://doi.org/10.1103/PhysRevB.81.064422)

PACS number(s): 75.30.Et, 75.30.Gw, 75.50.Ee, 76.30.—v

## I. INTRODUCTION

Recently, a considerable amount of attention has been devoted to the theoretical and experimental investigation of two-dimensional (2D) quantum spin systems. In case of the ideal 2D Heisenberg antiferromagnet (AF) on a square lattice, the magnetic long-range order is suppressed by zero-point fluctuations at any finite temperature.<sup>1</sup> However, the presence of an easy-axis anisotropy can induce a finite-temperature phase transition into the Néel ordered state.<sup>2</sup> On the other hand, for an easy-plane anisotropy, a Berezinskii-Kosterlitz-Thouless (BKT) transition<sup>3,4</sup> was proposed, where the high-temperature disordered phase can be described as a gas of vortices. Below the BKT transition ( $T_{\text{BKT}}$ ), the vortices are bound in vortex-antivortex pairs and the spin-spin correlation decay changes from exponential to algebraic.<sup>5</sup> A crossover from the isotropic to XY behavior in low fields has been predicted for 2D Heisenberg AF.<sup>6,7</sup>

Interplane interactions (which are always present in real materials) can significantly modify the ground-state properties of quasi-2D systems, inducing for instance a phase transition with three-dimensional (3D) long-range magnetic order. Due to the onset of 3D ordering in most real materials, the critical behavior of diverging quantities as anticipated for ideal 2D systems at  $T_{\text{BKT}}$  is hardly observable experimentally.

The quasi-2D Heisenberg AF model with interplane interactions can be described by the Hamiltonian

$$\mathcal{H} = J \sum_{\langle i,j \rangle_{ab}} \mathbf{S}_i \cdot \mathbf{S}_j + J' \sum_{\langle i,j \rangle_c} \mathbf{S}_i \cdot \mathbf{S}_j - \beta \sum_i S_i^z \quad (1)$$

with  $\beta = g\mu_B B$ , where  $\mu_B$  is the Bohr magneton,  $J$  and  $J'$  are the intraplane and interplane exchange interactions, respectively, and  $\langle i,j \rangle_{ab}$  and  $\langle i,j \rangle_c$  correspond to nearest-neighbor spin pairs formed in the directions parallel and perpendicular to the  $S=\frac{1}{2}$  planes, respectively. The variation in the ratio  $J'/J$  allows to study nicely the rich phase diagram of

quasi-2D magnetic systems, including the transition from a 2D Heisenberg AF ( $J'/J=0$ ) to the 3D Heisenberg AF ( $J'/J=1$ ). Remarkably, even in presence of relatively strong interplane interactions, the 2D quantum fluctuations can significantly affect the magnetic properties of such systems,<sup>8</sup> resulting, for instance, in a peculiar nonmonotonic field dependence of the ordering temperature. Such a behavior has recently been observed in the quasi-2D square-lattice Heisenberg AF  $[\text{Cu}(\text{C}_4\text{H}_4\text{N}_2)_2(\text{HF}_2)]\text{BF}_4$  (Refs. 8 and 9) and in the spatially anisotropic triangular magnet  $\text{Cu}(\text{tn})\text{Cl}_2$ ,<sup>10</sup> where tn is 1,3-diaminopropane ( $\text{C}_3\text{H}_{10}\text{N}_2$ ).

Here, we report on magnetic properties of single-crystalline samples of  $[\text{Cu}(\text{pyz})_2(\text{HF}_2)]\text{PF}_6$ , which is regarded as a nearly perfect realization of a quasi-2D  $S=\frac{1}{2}$  Heisenberg AF. Comprehensive specific heat, high-field magnetization, and electron-spin-resonance (ESR) studies allow us to identify a long-range ordered Néel state with easy-plane anisotropy and to accurately estimate the spin-Hamiltonian parameters. We show that in spite of the onset of the 3D ordered state below  $T_N$ , the magnetic properties of  $[\text{Cu}(\text{pyz})_2(\text{HF}_2)]\text{PF}_6$  are still significantly affected by 2D spin correlations.

## II. EXPERIMENTAL DETAILS

The measurements have been performed at the Dresden High Magnetic Field Laboratory (*Hochfeld-Magnetlabor Dresden*, HLD). The pulsed-field magnetization was obtained by integrating the voltage induced in a compensated pickup coil system containing a sample. The low-field magnetization below 7 T was measured using a commercial superconducting quantum interference device (SQUID) magnetometer. The specific-heat measurements were performed using a continuous relaxation-time technique.<sup>11,12</sup> For the X-band ESR measurements a Bruker ELEXSYS E500 spectrometer operating at a frequency of 9.4 GHz was used. The

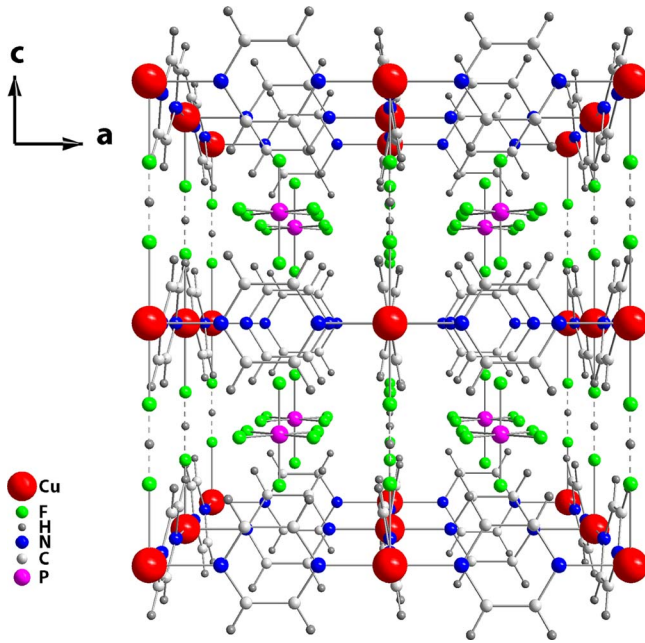


FIG. 1. (Color online) Structure of  $[\text{Cu}(\text{pyz})_2(\text{HF}_2)]\text{PF}_6$  viewed along the  $b$  axis.

ESR experiments in the frequency range 36–250 GHz were performed at temperatures down to 1.3 K using a tunable-frequency homemade ESR spectrometer (similar to that described in Ref. 13) equipped with a 16 T high-homogeneity superconducting magnet. In our experiments we used single crystals with a typical size of  $4 \times 3 \times 1$  mm<sup>3</sup>, synthesized by aqueous reaction of stoichiometric amounts of ammonium bifluoride, pyrazine, and copper (II) hexafluorophosphate hydrate (using the same procedure as reported in Refs. 9 and 14).

### III. RESULTS AND DISCUSSION

$[\text{Cu}(\text{pyz})_2(\text{HF}_2)]\text{PF}_6$ , where pyz is pyrazine ( $\text{C}_4\text{H}_4\text{N}_2$ ), crystallizes in a tetragonal lattice (space group  $P4/nmm$ ;  $Z = 1$ ). The structure consists of square-lattice planes of  $\text{Cu}^{2+}$  ions bridged by pyz groups in the  $ab$  plane (Fig. 1). The planes are connected by  $\text{HF}_2$  groups along the  $c$  axis. The planes of the pyz groups are nearly orthogonal to the  $\text{Cu}^{2+}$  planes. The noncoordinating  $\text{PF}_6$  groups pack in between the planes in the center of almost cubic units.<sup>15</sup>

The magnetization of  $[\text{Cu}(\text{pyz})_2(\text{HF}_2)]\text{PF}_6$  was measured at 1.5 K in magnetic fields up to 50 T applied parallel and perpendicular to the  $c$  axis (Fig. 2). The fully spin-polarized state was observed at  $B_c^{ab} = 37.5$  T and  $B_c^c = 33.8$  T for  $B \parallel ab$  and  $B \parallel c$ , respectively. In the scaled plot of Fig. 2, it becomes obvious that the magnetizations for different magnetic-field orientations coincide nicely. This means that the magnetization anisotropy is solely determined by the  $g$  factor anisotropy. The numerically calculated magnetization for an  $S = \frac{1}{2}$  2D square-lattice Heisenberg AF with an intraplane exchange interaction  $J/k_B = 12.8$  K (Refs. 15 and 16) is in very good agreement with our data (Fig. 2). In order to estimate the ratio  $J'/J$ , calculations using this model with different

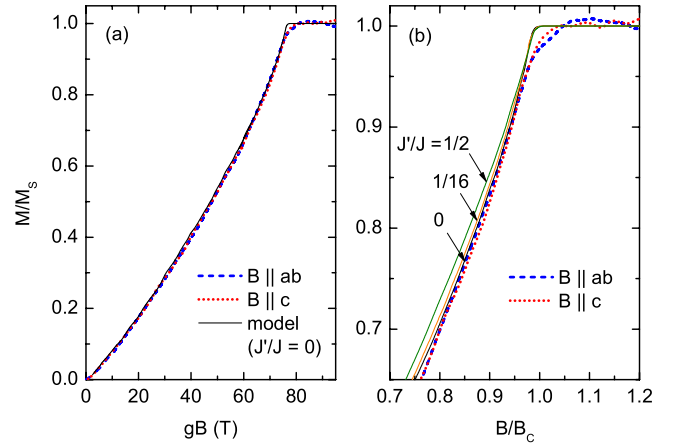


FIG. 2. (Color online) (a) High-field magnetization of  $[\text{Cu}(\text{pyz})_2(\text{HF}_2)]\text{PF}_6$  (dashed and dotted lines correspond to  $B \parallel ab$  and  $B \parallel c$ , respectively) as a function of  $gB$ , where  $B$  is the applied magnetic field and the  $g$  factors are  $g_c = 2.28$  and  $g_{ab} = 2.05$ , as determined by X-band ESR measurements. The calculated magnetization for an  $S = \frac{1}{2}$  2D square-lattice Heisenberg AF is shown by the solid line. (b) The same data in an expanded scale close to saturation with additional model calculations assuming a finite interplane interaction.

interplane interactions have been made [Fig. 2(b)].<sup>15</sup> By comparison with our data it can be concluded that  $J'/J$  must be less than  $1/16$ .

The high-resolution specific-heat measurements allowed to clearly resolve the 3D AF ordering temperature in zero and applied magnetic fields up to 14 T [Fig. 3(a)]. Using the local maximum of the specific-heat anomaly, the  $B$ - $T$  phase diagram has been extracted. Figure 3(b) shows the result together with data calculated for an ideal 2D Heisenberg AF system ( $J' = 0$ ) with  $J/k_B = 12.8$  K.<sup>8</sup> The theory<sup>7,8</sup> predicts that an applied magnetic field suppresses fluctuations of the spin  $z$  component. As a result, an effective easy-plane anisotropy is induced in the system, accompanied by the rise of  $T_N$ . On the other hand, for sufficiently strong magnetic field, the spin-canting effect prevails. Then, the critical temperature decreases and vanishes eventually at the saturation field, when the fully spin-polarized state is reached. The measured nonmonotonic  $B$ - $T$  phase diagram of  $[\text{Cu}(\text{pyz})_2(\text{HF}_2)]\text{PF}_6$  can be nicely explained by modifying above model with a weak interplane interaction. As a threshold for the observation of a  $\lambda$ -like anomaly in the specific heat,  $J'/J < 0.015$  has been given in Ref. 17. This ratio is very close to that,  $J'/J = 0.01$ , estimated from previous experiments on powdered samples.<sup>15</sup>

In the range  $0.001 \leq J'/J \leq 1$  the interplane coupling can be estimated employing the following formula:<sup>18</sup>

$$T_N = 4\pi\rho_S[2.43 - \ln(J'/J)], \quad (2)$$

where  $\rho_S = 0.183J$  is the spin stiffness for a 2D system. Using the exchange coupling, obtained from the high-field magnetization data, and  $T_N = 4.38$  K we find  $J'/J = 0.014$ , which is in excellent agreement with our previous estimate.

ESR is a powerful technique to determine the magnetic structure and the effective spin-Hamiltonian parameters of in

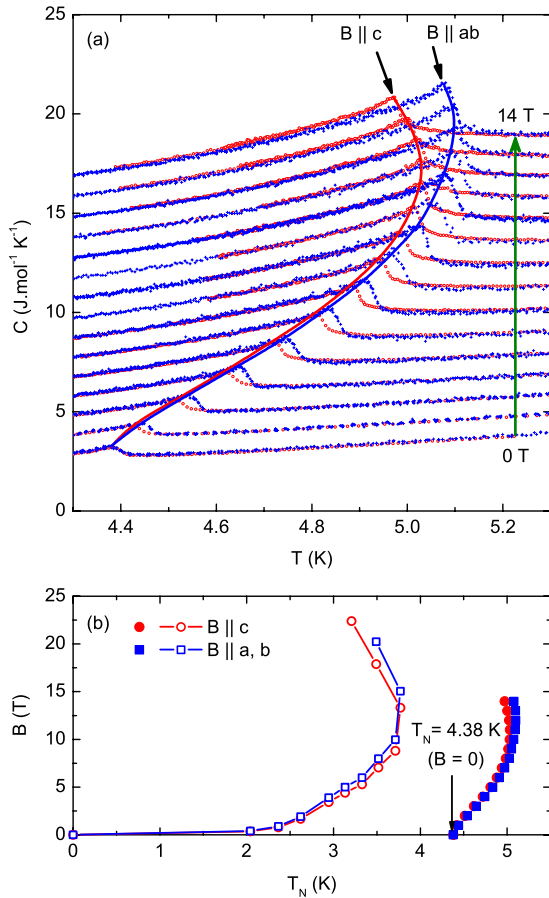


FIG. 3. (Color online) (a) Temperature dependence of the specific heat of  $[\text{Cu}(\text{pyz})_2(\text{HF}_2)]\text{PF}_6$  for  $B \parallel ab$  (blue crosses) and  $B \parallel c$  (red circles). The experimental data are shifted by  $1 \text{ J mol}^{-1} \text{ K}^{-1} \text{ T}^{-1}$ . (b) The  $B$ - $T$  phase diagram of  $[\text{Cu}(\text{pyz})_2(\text{HF}_2)]\text{PF}_6$  obtained from the specific-heat data (full symbols) shown together with the calculated phase diagram for the ideal 2D case with  $J' = 0$  (open symbols) (Ref. 8). Lines are guides to the eye.

exchange-coupled spin systems. Low-frequency ESR data on  $[\text{Cu}(\text{pyz})_2(\text{HF}_2)]\text{PF}_6$  were reported previously.<sup>19</sup> In our work the frequency range of ESR measurements was extended up to 260 GHz. The application of the tunable-frequency ESR technique allowed us to observe the energy gap in the AF ordered state of this compound directly and estimate the anisotropy constant. At room temperature, a single ESR line was observed for all field orientations with a typical sinusoidal angular dependence of the  $g$  factor expected for a  $\text{Cu}^{2+}$  ion in an octahedral surrounding with an axial symmetry due to the Jahn-Teller effect. The results confirm that the main exchange paths between the magnetic ions are formed in the  $ab$  planes by  $d_{x^2-y^2}$  orbitals,<sup>20</sup> which directly overlap with orbitals of pyrazine ligands, creating a quasi-2D network of exchange-coupled  $\text{Cu}^{2+}$  ions.

The temperature evolution of the ESR spectra in  $[\text{Cu}(\text{pyz})_2(\text{HF}_2)]\text{PF}_6$  measured at 90 GHz for  $B \parallel c$  is shown in Fig. 4. The temperature dependence of the resonance field, the linewidth, and the integrated intensity of the ESR lines in fields applied parallel and perpendicular to the  $ab$  plane are shown in Figs. 5(a), 5(b), and 6. It is evident that in the

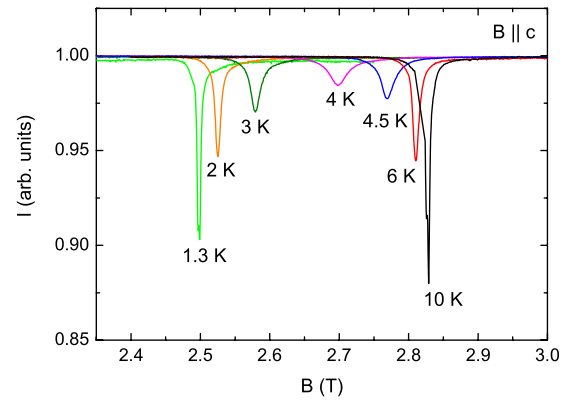


FIG. 4. (Color online) ESR signal (transmission) measured at 90 GHz in a temperature range of 1.3–10 K for  $B \parallel c$ .

vicinity of the ordering temperature ( $T_N \approx 4.6 \text{ K}$  at 3 T), a region of enhanced short-range spin correlations is entered and both the resonance field and the linewidth change dramatically. It is important to mention that the integrated ESR intensity is proportional to the dynamic spin susceptibility. In Fig. 6, the temperature dependence of  $M/B$  (measured using a SQUID magnetometer with applied magnetic field  $B = 3 \text{ T}$ ), the integrated ESR intensity, and the magnetic susceptibility calculated for a 2D Heisenberg AF system<sup>16,21</sup> are presented. The results of the calculations are in good agreement with our experimental data above  $T_N$  for  $J/k_B = 12.8 \text{ K}$ , proving the crucial role of 2D spin correlations in  $[\text{Cu}(\text{pyz})_2(\text{HF}_2)]\text{PF}_6$ .

The frequency-field diagram of the ESR signals is presented in Fig. 7. Well above the critical temperature ( $T = 15 \text{ K}$ ), we observe only one resonance mode for each orientation,  $B \parallel c$  and  $B \parallel ab$ , as shown in the inset of Fig. 7.

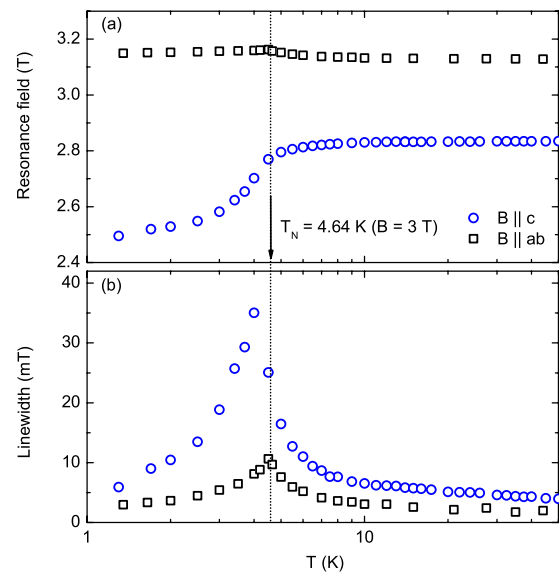


FIG. 5. (Color online) Temperature dependence of the (a) resonance field and (b) linewidth obtained from ESR data measured at  $\nu = 90 \text{ GHz}$  for a magnetic field aligned parallel (empty squares) and perpendicular (empty circles) to the  $ab$  plane. The transition temperature,  $T_N = 4.64 \text{ K}$ , as obtained from specific-heat measurements at 3 T for  $B \parallel ab$  (Fig. 3) is shown by the dotted line.

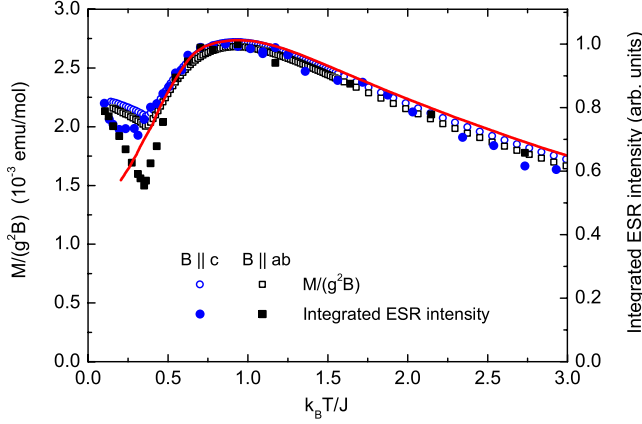


FIG. 6. (Color online) Temperature dependence of  $M/B$  measured at  $B=3$  T (open symbols) and the integrated intensity obtained from ESR data measured at  $\nu=90$  GHz (full symbols). The data are presented together with the calculated results (solid line) for a 2D square-lattice Heisenberg AF system with  $J/k_B=12.8$  K (Refs. 16 and 21).

The frequency-field dependence of these modes corresponds to transitions between the energy levels of the  $S=\frac{1}{2}$   $\text{Cu}^{2+}$  ions and can be described by  $h\nu=g\mu_B B$  with  $g_c=2.28$  and  $g_{ab}=2.05$ .

The ESR excitation spectrum changes dramatically below  $T_N$ , as shown for  $T=1.3$  K in Fig. 7. Two modes,  $\omega_1$  and  $\omega_2$ , are observed when the magnetic field is applied in the  $ab$  plane. For  $B||c$ , a nonlinear dependence of the mode  $\omega_4$  was observed. Most importantly, in the ESR excitation spectrum the AF resonance gap was determined by us directly,  $\Delta=43$  GHz ( $\approx 2$  K) at  $B=0$ . Such a frequency-field diagram is a textbook example for magnetic excitations in a system with collinear 3D AF long-range order and easy-plane anisotropy.<sup>22</sup> The frequency-field dependence of the antiferromagnetic resonance modes can be calculated using the mean-field approximation<sup>23</sup>

$$\omega_1/\gamma = B, \quad (3)$$

$$\omega_2/\gamma = \sqrt{2B_A B_E - (B_A/2B_E)B^2}, \quad (4)$$

for magnetic fields applied parallel to the easy plane and

$$\omega_3/\gamma = 0, \quad (5)$$

$$\omega_4/\gamma = \sqrt{2B_A B_E + (1 - B_A/2B_E)B^2}, \quad (6)$$

for magnetic fields applied perpendicular to the easy plane, where  $\gamma=g\mu_B/\hbar$  is the gyromagnetic ratio, and  $B_E$  and  $B_A$  are the exchange and anisotropy field, respectively. Our results clearly show that below  $T_N$ , the  $ab$  plane is the easy plane along which the magnetic moments are aligned at  $B=0$ . The frequency-field diagram was analyzed using Eqs. (3)–(6). The best fit was obtained for  $B_E=18.72$  T and  $B_A=0.05$  T. The exchange field,  $B_E$ , is related to the exchange coupling by the simple relation  $B_E=4SJ/\hbar\gamma$  and yields

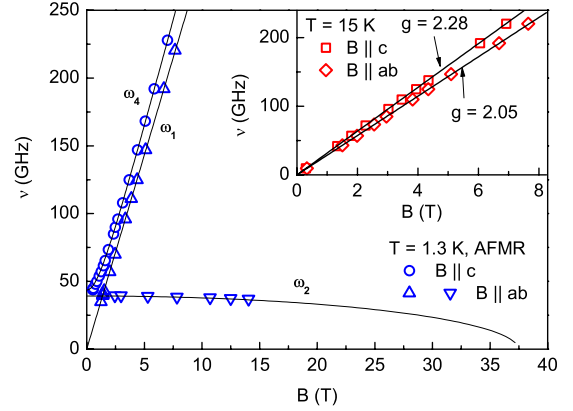


FIG. 7. (Color online) Frequency-field diagram of the ESR excitations measured at  $T=1.3$  K for a magnetic field aligned parallel (triangles) and perpendicular (circles) to the  $ab$  plane. The signals  $\omega_1$ ,  $\omega_2$ , and  $\omega_4$  correspond to AF resonance modes of a 3D ordered AF system with easy-plane anisotropy calculated as described in the text. The inset shows the ESR modes observed above the ordering temperature. These modes can be described as transitions between the energy levels of  $\text{Cu}^{2+}$  ions by the equation  $h\nu=g\mu_B B$ .

$J/k_B=12.9$  K, which is in perfect agreement with the value of the intraplane exchange coupling obtained from our magnetization and specific-heat measurements. Noticeably, using ESR data, the anisotropy constant ( $\sim 0.3\%$  of the exchange interaction) can be estimated, revealing the validity of isotropic quasi-2D  $S=\frac{1}{2}$  Heisenberg model applied to  $[\text{Cu}(\text{pyz})_2(\text{HF}_2)]\text{PF}_6$ .

#### IV. CONCLUSION

Our comprehensive specific heat, high-field magnetization, and ESR studies revealed the important role of 2D spin correlations on the magnetic properties of the  $S=\frac{1}{2}$  quasi-2D Heisenberg AF  $[\text{Cu}(\text{pyz})_2(\text{HF}_2)]\text{PF}_6$ . The observation of two AF resonance modes below  $T_N$  confirms the presence of a 3D collinear AF long-range ordered state with an energy gap of  $\Delta=43$  GHz in the magnetic excitation spectrum and  $A/J\sim 0.003$  for the anisotropy/exchange interaction ratio. The presence of a field-induced XY behavior has unambiguously been identified by the observation of a peculiar non-monotonic field dependence of the ordering temperature.

#### ACKNOWLEDGMENTS

This work has been supported by Deutsche Forschungsgemeinschaft, EuroMagNET (EU under Contract No. 228043), and UChicago Argonne, LLC, Operator of Argonne National Laboratory (“Argonne”). Argonne, a U.S. Department of Energy, Office of Science Laboratory, is operated under Contract No. DE-AC02-06CH11357. E.Č. is supported also by APVV under Grant No. APVV-VVCE-0058-07 and VEGA under Grant No. 1/0078/09. We would like to thank L. Zviagina for preparations of pulse-field magnetization measurements.



- <sup>1</sup>N. Mermin and H. Wagner, Phys. Rev. Lett. **17**, 1133 (1966).
- <sup>2</sup>A. Cuccoli, T. Roscilde, V. Tognetti, R. Vaia, and P. Verrucchi, Phys. Rev. B **67**, 104414 (2003).
- <sup>3</sup>V. L. Berezinskii, Zh. Eksp. Teor. Fiz. **59**, 907 (1970); **61**, 1144 (1971).
- <sup>4</sup>J. M. Kosterlitz and D. J. Thouless, J. Phys. C **5**, L124 (1972); **6**, 1181 (1973).
- <sup>5</sup>R. Gupta and C. F. Baillie, Phys. Rev. B **45**, 2883 (1992).
- <sup>6</sup>A. S. T. Pires, Phys. Rev. B **50**, 9592 (1994).
- <sup>7</sup>A. Cuccoli, T. Roscilde, R. Vaia, and P. Verrucchi, Phys. Rev. B **68**, 060402(R) (2003).
- <sup>8</sup>P. Sengupta, C. D. Batista, R. D. McDonald, S. Cox, J. Singleton, L. Huang, T. P. Papageorgiou, O. Ignatchik, T. Herrmannsdörfer, J. L. Manson, J. A. Schlueter, K. A. Funk, and J. Wosnitza, Phys. Rev. B **79**, 060409(R) (2009).
- <sup>9</sup>J. L. Manson, M. M. Conner, J. A. Schlueter, T. Lancaster, S. J. Blundell, M. L. Brooks, F. L. Pratt, T. Papageorgiou, A. D. Bianchi, J. Wosnitza, and M.-H. Whangbo, Chem. Commun. (Cambridge) **2006**, 4894.
- <sup>10</sup>A. Orendáčová, E. Čížmár, L. Sedláková, J. Hanko, M. Kajňáková, M. Orendáč, A. Feher, J. S. Xia, L. Yin, D. M. Pajerowski, M. W. Meisel, V. Zeleňák, S. Zvyagin, and J. Wosnitza, Phys. Rev. B **80**, 144418 (2009).
- <sup>11</sup>Y. Wang, T. Plackowski, and A. Junod, Physica C **355**, 179 (2001).
- <sup>12</sup>R. Lortz, Y. Wang, A. Demuer, P. H. M. Böttger, B. Bergk, G. Zwicknagl, Y. Nakazawa, and J. Wosnitza, Phys. Rev. Lett. **99**, 187002 (2007).
- <sup>13</sup>S. A. Zvyagin, J. Krzystek, P. H. M. van Loosdrecht, G. Dhalenne, and A. Revcolevschi, Physica B **346-347**, 1 (2004).
- <sup>14</sup>J. L. Manson, J. A. Schlueter, K. A. Funk, H. I. Southerland, B. Twamley, T. Lancaster, S. J. Blundell, P. J. Baker, F. L. Pratt, J. Singleton, R. D. McDonald, P. A. Goddard, P. Sengupta, C. D. Batista, L. Ding, C. Lee, M.-H. Whangbo, I. Franke, S. Cox, C. Baines, and D. Trial, J. Am. Chem. Soc. **131**, 6733 (2009).
- <sup>15</sup>P. A. Goddard, J. Singleton, P. Sengupta, R. D. McDonald, T. Lancaster, S. J. Blundell, F. L. Pratt, S. Cox, N. Harrison, J. L. Manson, H. I. Southerland, and J. A. Schlueter, New J. Phys. **10**, 083025 (2008).
- <sup>16</sup>F. M. Woodward, A. S. Albrecht, C. M. Wynn, C. P. Landee, and M. M. Turnbull, Phys. Rev. B **65**, 144412 (2002).
- <sup>17</sup>P. Sengupta, A. W. Sandvik, and R. R. P. Singh, Phys. Rev. B **68**, 094423 (2003).
- <sup>18</sup>C. Yasuda, S. Todo, K. Hukushima, F. Alet, M. Keller, M. Troyer, and H. Takayama, Phys. Rev. Lett. **94**, 217201 (2005).
- <sup>19</sup>S. Cox, R. D. McDonald, J. Singleton, S. Miller, P. A. Goddard, S. El Shawish, J. Bonca, J. A. Schlueter, and J. L. Manson, arXiv:0907.3514 (unpublished).
- <sup>20</sup>A. Abragam and B. Bleaney, *Electron Paramagnetic Resonance of Transition Ions* (Clarendon, Oxford, 1970).
- <sup>21</sup>Y. J. Kim and R. J. Birgeneau, Phys. Rev. B **62**, 6378 (2000).
- <sup>22</sup>E. A. Turov, *Physical Properties of Magnetically Ordered Crystals* (Academic, New York, 1965).
- <sup>23</sup>J. W. Battles and G. E. Everett, Phys. Rev. B **1**, 3021 (1970).